

# Acclimation to Fluctuating Light Impacts the Rapidity of Response and Diurnal Rhythm of Stomatal Conductance<sup>1</sup>[CC-BY]

Jack S.A. Matthews,<sup>2</sup> Silvere Vialet-Chabrand,<sup>2</sup> and Tracy Lawson<sup>3</sup>

School of Biological Sciences, University of Essex, Colchester CO4 3SQ, United Kingdom

ORCID IDs: 0000-0002-7282-8929 (J.S.A.M.); 0000-0002-2105-2825 (S.V.-C.); 0000-0002-4073-7221 (T.L.).

Plant acclimation to growth light environment has been studied extensively; however, the majority of these studies have focused on light intensity and photo-acclimation, with few studies exploring the impact of dynamic growth light on stomatal acclimation and behavior. To assess the impact of growth light regime on stomatal acclimation, we grew *Arabidopsis* (*Arabidopsis thaliana*) plants in three different lighting regimes (with the same average daily intensity), fluctuating with a fixed pattern of light, fluctuating with a randomized pattern of light (sinusoidal), and nonfluctuating (square wave), to assess the effect of light regime dynamics on gas exchange. We demonstrated that  $g_s$  (stomatal conductance to water vapor) acclimation is influenced by both intensity and light pattern, modifying the stomatal kinetics at different times of the day and resulting in differences in the rapidity and magnitude of the  $g_s$  response. We also describe and quantify the response to an internal signal that uncouples variation in  $A$  and  $g_s$  over the majority of the diurnal period and represents 25% of the total diurnal  $g_s$ . This  $g_s$  response can be characterized by a Gaussian element and when incorporated into the widely used Ball-Berry model greatly improved the prediction of  $g_s$  in a dynamic environment. From these findings, we conclude that acclimation of  $g_s$  to growth light could be an important strategy for maintaining carbon fixation and overall plant water status and should be considered when inferring responses in the field from laboratory-based experiments.

Despite typically occupying only 0.3% to 5% of the leaf surface, stomata control ~95% of all gas exchange between the external environment and leaf interior, and it has been estimated that 60% of all precipitation that falls on terrestrial ecosystems is taken up by plants and transpired through stomatal pores (Morison, 2003; Katul et al., 2012). With the global population continuing to rise and the need for increased crop yields, the excessive allocation of water to agriculture, currently sitting at ~70% to 90% of all globally available fresh water (Morison et al., 2008), highlights the need for sustainable crops with higher water use efficiency and lower inputs of water.

Stomatal behavior regulates CO<sub>2</sub> uptake for photosynthesis and water loss via transpiration (which is also important for regulating leaf temperature). The balance between these two fluxes can be characterized by intrinsic water use efficiency ( $W_i$ ), the ratio between CO<sub>2</sub> assimilation ( $A$ ), and stomatal conductance to water

vapor ( $g_s$ ). Low  $g_s$  can restrict CO<sub>2</sub> uptake into the leaf, thereby reducing  $A$  (Farquhar and Sharkey, 1982; Barradas et al., 1994; McAusland et al., 2016), whereas high  $g_s$  enables higher rates of  $A$  but at a greater cost of water loss via transpiration (Kirschbaum et al., 1988; Tinoco-Ojanguren and Percy, 1993; Jones, 1998; Lawson et al., 2010; Lawson and Blatt, 2014). To maintain an optimal balance between  $A$  and  $g_s$ , stomata continually adjust aperture to external environmental cues (e.g. photosynthetic photon flux density [PPFD]) and internal signals, which can include hormonal (e.g. abscisic acid [ABA]; Mencuccini et al., 2000; Tallman, 2004), circadian (Gorton et al., 1989, 1993; Dodd et al., 2005; Hubbard and Webb, 2015; Hassidim et al., 2017), and/or a currently unidentified mesophyll signal (Lee and Bowling, 1992; Mott et al., 2008; Fujita et al., 2013; Matthews et al., 2017). Many studies have reported a strong correlation between  $A$  and  $g_s$  (Wong et al., 1979), and it has been theorized that synchronicity exists to optimize the trade-off between photosynthesis and water loss (Buckley, 2017). However, this synchronicity is often constrained by the temporal stomatal response (Lawson and Blatt, 2014), that is the speed at which stomata open and close to changing environmental cues, such as those experienced in a dynamic field environment (Jones, 2013; Lawson et al., 2010; McAusland et al., 2016; Vialet-Chabrand et al., 2017a). Stomatal responses to changing environmental cues are often an order of magnitude slower than those observed in  $A$  (Tinoco-Ojanguren and Percy, 1993; Lawson et al., 2010; McAusland et al., 2016), resulting in lags in stomatal behavior and a temporal disconnect between

<sup>1</sup> J.S.A.M. is funded by a PhD Natural Environment Research Council DTP studentship (Env-East DTP E14EE). S.V.-C. was supported through Biotechnology and Biological Sciences Research Council grants BB/1001187/1 and BB/N021061/1 awarded to T.L.

<sup>2</sup> These authors contributed equally to the article.

<sup>3</sup> Address correspondence to [tlawson@essex.ac.uk](mailto:tlawson@essex.ac.uk).

The author responsible for distribution of materials integral to the findings presented in this article in accordance with the policy described in the Instructions for Authors ([www.plantphysiol.org](http://www.plantphysiol.org)) is: Tracy Lawson ([tlawson@essex.ac.uk](mailto:tlawson@essex.ac.uk)).

[CC-BY] Article free via Creative Commons CC-BY 4.0 license.

[www.plantphysiol.org/cgi/doi/10.1104/pp.17.01809](http://www.plantphysiol.org/cgi/doi/10.1104/pp.17.01809)

$A$  and  $g_s$ , with implications for water use efficiency and crop productivity (Lawson et al., 2010; Lawson and Blatt, 2014; McAusland et al., 2013, 2016). The close relationship between  $A$  and  $g_s$  has often been reported under steady-state conditions and has been used by many models to predict diurnal time courses of  $g_s$  (Damour et al., 2010), such as the widely used Ball-Berry model (Ball et al., 1987) and its derivatives. The use of steady-state models under fluctuating environmental conditions can lead to inaccurate predictions of the diurnal response of  $g_s$ , as these models do not really take into account the slow temporal response of stomata (Viale-Chabrand et al., 2013, 2017a; Matthews et al., 2017). Moreover, the lack in temporal synchronicity between  $A$  and  $g_s$  that cannot be predicted by these models has important implications for carbon gain and water use when integrated over the diurnal period and/or entire growing season. Furthermore, as measurements of  $g_s$  in the field are highly variable, they correlate poorly with those measured under steady state conditions in the laboratory (Poorter et al., 2016; Viale-Chabrand et al., 2017a), which are often taken in the middle of the day to maximize  $A$  and  $g_s$ . In addition to the temporal responses outlined above, diurnal variation in sensitivity and temporal kinetics to various stimuli have been reported for both stomatal behavior and photosynthesis. For example, there is evidence to suggest that the rapidity of stomatal responses may change at different times of day (Mencuccini et al., 2000; Tallman, 2004). Additionally, changes in  $g_s$  to fluctuations in water status have been shown to restrict  $A$  depending on the time of day, and stomata have been reported to be more responsive to ABA in the morning compared with the afternoon (Mencuccini et al., 2000). It has been recognized that the circadian clock at least in part controls these diurnal modifications in  $A$  and  $g_s$  responses over the diurnal period (Dodd et al., 2005; Hassidim et al., 2017), through regulating the temporal patterns of transcription in photosynthesis, stomatal opening, and other physiological processes (Gorton et al., 1989, 1993; Hubbard and Webb, 2015). Phase adjustment of the circadian clock to environmental cues such as light or temperature is fundamental for synchronizing plant biological processes with growth environment (Yin and Johnson, 2000; Resco de Dios et al., 2016), which is important for photosynthesis and plant growth (Dodd et al., 2005; Caldeira et al., 2014). However, there is also evidence, in *Arabidopsis*, that endogenous signals such as accumulated photosynthates provide feedback mechanisms that regulate the clock phase, and that these are essential for regulating carbon metabolism in dynamic light environments (Seki et al., 2017; Resco de Dios et al., 2016; Ohara and Satake, 2017; Haydon et al., 2017). Although the mechanism(s) behind diurnal regulation of  $A$  and  $g_s$  and the impact on water use efficiency are not fully understood, these studies highlight the need for a greater understanding of the impact of temporal stomatal response over the entire diurnal period, as these will have important implications for cumulative  $A$  and water loss as well as model predictions.

The speed and magnitude of the temporal response of  $g_s$  is known to vary between species (McAusland et al., 2016), although little is known about how growth light conditions may affect stomatal responses at different times of the day. In the natural environment, the response of  $A$  and  $g_s$  is dominated by PPFD (Percy, 1990; Way and Percy, 2012), which varies temporally over the course of seconds, minutes, days, and seasons (Assmann and Wang, 2001) due to changes in cloud cover, sun angle, and shading from neighboring leaves and plants (Percy, 1990; Chazdon and Percy, 1991; Way and Percy, 2012). Leaves therefore experience short- and long-term fluctuations in light (sun/shade flecks) to which  $g_s$  and  $A$  respond. Although it is well established that photosynthesis and to some extent stomatal behavior (including  $g_s$  kinetics) acclimate to growth PPFD intensity, we have recently demonstrated that photosynthesis acclimates to the pattern of growth irradiance as well as intensity (Viale-Chabrand et al., 2017b), with fluctuating light having a large impact on photosynthetic performance (Külheim et al., 2002; Alter et al., 2012; Suorsa et al., 2012; Kromdijk et al., 2016; Yamori 2016; Kaiser et al., 2016, 2017a; Viale-Chabrand et al., 2017b). Additionally, a recent study by Kaiser et al. (2017b) demonstrated that leaf gas exchange acclimates to light flecks; however, as growth light was kept constant this study focused on dynamic acclimation of photosynthesis. It is not currently known if fluctuations in light impact stomatal acclimation (as well as  $A$ ) and potentially influence the magnitude and temporal dynamics of  $g_s$  and  $A$  over the diurnal period. To assess the influence of dynamic light on temporal kinetics and diurnal responses of  $g_s$  and  $A$ , we compared gas exchange in *Arabidopsis* plants (Col-0) grown under dynamic light that mimics the field environment, with plants grown under square wave light regimes, representative of laboratory growth conditions. We used controlled growth light environments to acclimate plants to different light regimes, while maintaining the same time integrated daily light intensity. Plants were grown under three light regimes—fluctuating with a fixed pattern of light, fluctuating with a randomized pattern of light (sinusoidal), and nonfluctuating (square wave)—to assess the effect of light pattern on gas exchange. Two different average light intensities (high and low) were used to separate the effect of light intensity from light pattern on stomatal acclimation and response.

To evaluate the impact of  $g_s$  acclimation to growth light conditions, we assessed the response of  $g_s$  to a step change in light as well as the diurnal response of  $g_s$  under constant light. This allowed us to quantify the periodicity, magnitude, and rapidity of the response of  $g_s$  and determine if these processes significantly impact stomatal behavior over the course of the day. To separate the response of  $g_s$  from environmental/external and nonenvironmental/internal signals, gas exchange measurements of  $A$  and  $g_s$  were captured over a 12-h period under a constant square wave light regime. As a result, any variation in the response of  $g_s$  will be due to

the acclimatory response of internal signals to the pattern of growth light. When used in conjunction with current steady-state models of  $g_s$ , a better understanding of the  $g_s$  response to internal signals could greatly improve their predictive power. Our approach for quantifying the diurnal response of  $g_s$  could prove useful for rapidly quantifying the influence of circadian or diurnal elements relative to external signals in a dynamic environment.

## RESULTS

### Diurnal Responses of $g_s$ , $A$ , and $W_i$ to a Square Wave Pattern of Light

To investigate the acclimation of diurnal stomatal responses in plants grown under the six light treatments (FLH, fluctuating high light; SNH, sinusoidal high light; SQH, square high light; FLL, fluctuating low light; SNL, sinusoidal low light; SQL, square low light), all treatments were subjected to the square wave light regime corresponding to their growth light intensity ( $SQ_{High}$  high-light treatments;  $SQ_{Low}$  low-light treatments), with  $A$  (Fig. 1A),  $g_s$  (Fig. 1B), and  $W_i$  (Fig. 1C) measured continuously over the diurnal period. When integrated over the entire diurnal period,  $A$  was higher in SQH grown plants compared to FLH and significantly higher (posthoc Tukey,  $P < 0.05$ ) in SQH- compared to

SNH-grown plants (Fig. 1A), although there was no difference between plants under low-light treatments. After  $\sim 5$  h into the light regime,  $A$  started to decrease in all high-light-grown plants, and this decrease continued to the end of the light period (Fig. 1A). In all low-light treatments, a continuous slow decrease in  $A$  was observed throughout the entire diurnal light period. In all growth light treatments,  $g_s$  responses were not coordinated with  $A$  and displayed a Gaussian pattern of response (Fig. 1B), while  $A$  displayed a more square wave response (Fig. 1A). FLH-, SQH-, and SNH-grown plants displayed similar patterns of  $g_s$  but differed in the maximum  $g_s$  achieved and the time at which peak  $g_s$  occurred over the diurnal period. Initial levels of  $g_s \sim 1$  h after the light was turned on were comparable between all treatments dependent on light intensity, while maximum values of  $g_s$  in all treatments were reached  $\sim 4.5$  to 6 h into the diurnal period (Fig. 1B). In the evening (6–8 pm)  $g_s$  decreased to a value  $\sim 0.06 \text{ mol m}^{-2} \text{ s}^{-1}$  lower than the initial value observed in the morning in SQH and FLH treatments ( $\sim 0.3$  to  $0.24 \text{ mol m}^{-2} \text{ s}^{-1}$ , morning and evening, respectively), although this was not the case in SNH ( $0.27$  to  $0.26 \text{ mol m}^{-2} \text{ s}^{-1}$ ) grown plants. The maximum value of  $g_s$  reached during the diurnal period was higher in FLH ( $0.38 \text{ mol m}^{-2} \text{ s}^{-1}$ ) and SNH ( $0.375 \text{ mol m}^{-2} \text{ s}^{-1}$ ) compared to SQH ( $0.32 \text{ mol m}^{-2} \text{ s}^{-1}$ ) grown plants (Fig. 1B). FLL and SNL showed higher levels of  $g_s$  than SQL-grown plants throughout the day,

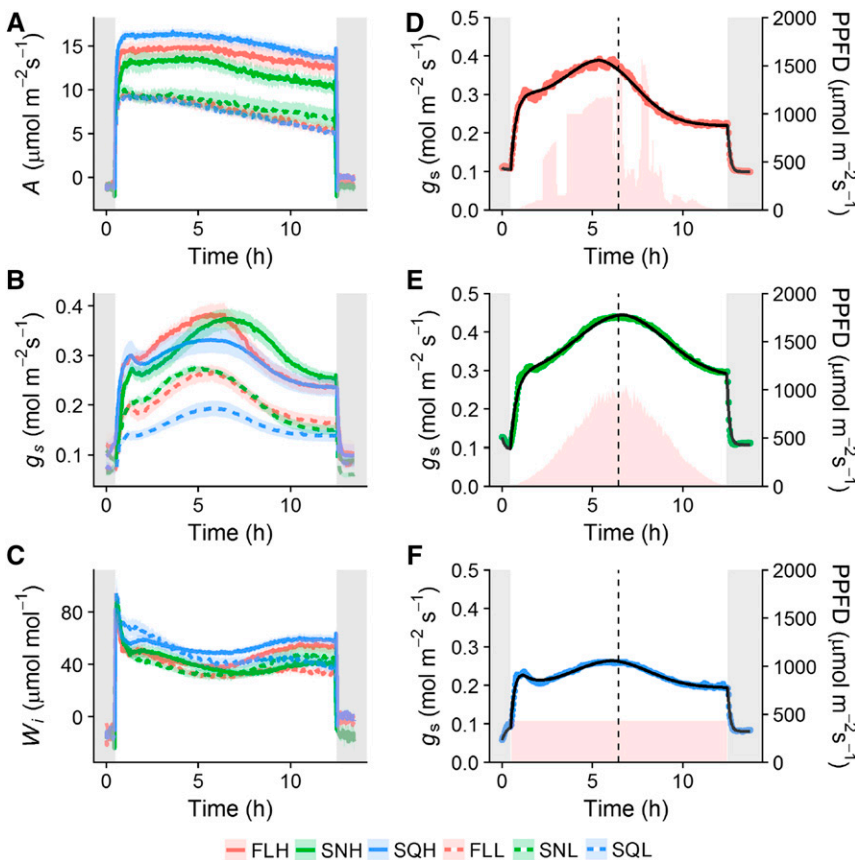


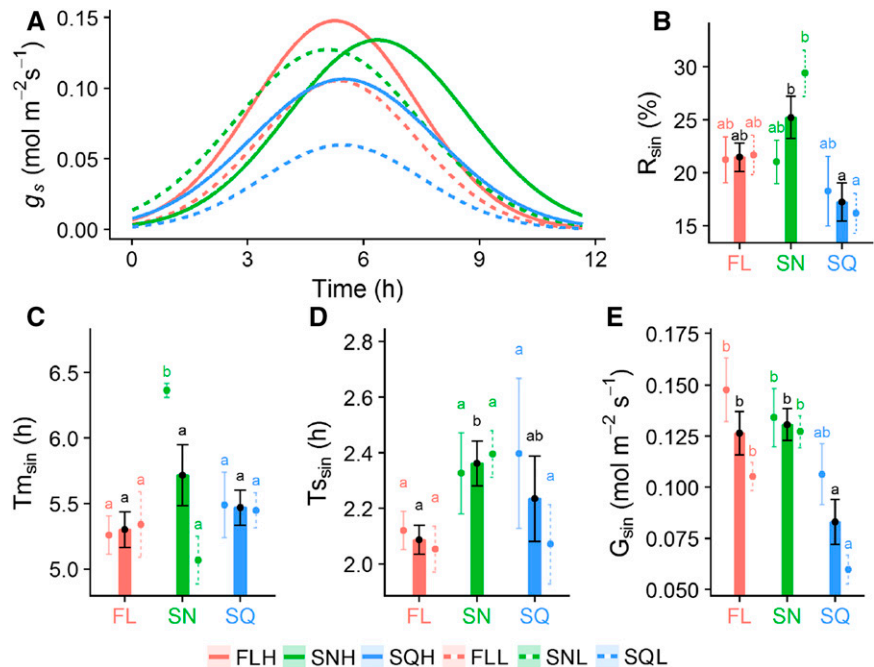
**Figure 1.** Diurnal measurements of  $A$ ,  $g_s$ , and  $W_i$  measured under square wave regimes of light. FLH (red), SNH (green), and SQH (blue) high-light treatments (full lines) were measured under  $SQ_{High}$ . FLL (red), SNL (green), and SQL (blue) low-light treatments (dashed lines) were measured under  $SQ_{Low}$ . Error bars represent mean  $\pm$  SE,  $n = 5-7$ . Gray shaded areas indicate when light source is off. Represented are examples of FLH (D), SNH (E), and SQH (F) to highlight fit of the temporal response exponential model (black line). Pink shaded areas illustrate growth light regimes for FLH (D), SNH (E), and SQH (F).

with the maximum  $g_s$  reached significantly higher (posthoc Tukey,  $P < 0.05$ ) in FLL ( $0.27 \text{ mol m}^{-2} \text{ s}^{-1}$ ) and SNL ( $0.275 \text{ mol m}^{-2} \text{ s}^{-1}$ ) compared to SQL ( $0.19 \text{ mol m}^{-2} \text{ s}^{-1}$ ) grown plants (Fig. 1B).  $W_i$  was greater in SQH-grown plants compared to FL and SN treatments across the entire diurnal light period, in both high- and low-light-grown plants measured under their respective light intensities (Fig. 1C). When integrated over the entire diurnal period,  $W_i$  was significantly higher ( $P < 0.05$ ) in SQH compared to SNH grown plants (data not shown). In high-light treatments,  $W_i$  remained relatively constant between morning and evening, assisted by the fact that the decrease in  $A$  toward the end of the day was accompanied by a decrease in  $g_s$ . In low-light treatments,  $W_i$  decreased through the day driven by the continuous slow decrease in  $A$ . All six treatments experienced a drop in  $W_i$  at midday due to the increase of  $g_s$  at this time, with little or no change in  $A$  (Fig. 1C). The temporal response of  $g_s$  to external and internal cues was modeled using an exponential equation (Eq. 2; see "Materials and Methods"). Figure 1, D to F, display examples of the model fit on individuals of each high-light treatment (FLH, SNH, and SQH, respectively).  $R^2$  and  $rmse$  of the relationship between observed, and predicted data were as follows for all treatments ( $R^2$  and  $rmse$ , respectively): FLH (0.99, 0.008), SNH (0.99, 0.008), SQH (0.99, 0.005), FLL (0.99, 0.006), SNL (0.99, 0.006), and SQL (0.99, 0.002).

To further characterize the importance of the Gaussian response of  $g_s$  relative to the diurnal variation, we used a descriptive model to dissect the data into parameters that relate to variation of the leaf internal signals. Using this model, we separated the Gaussian element of the diurnal response of  $g_s$  from the response

to change in light intensity (Fig. 2A), and determined the percentage of Gaussian driven  $g_s$  ( $R_{sin}$ , Fig. 2B), the time at which peak  $g_s$  occurs ( $Tm_{sin}$ , Fig. 2C), the width of the peak ( $Ts_{sin}$ , Fig. 2D), and magnitude of the Gaussian  $g_s$  response ( $G_{sin}$ , Fig. 2E). Significant differences in  $R_{sin}$  (Fig. 2B) were observed between plants grown under different light regimes (posthoc Tukey,  $P < 0.05$ ), with the lowest values  $\sim 16\%$  observed in SQL grown plants and the highest  $\sim 30\%$  in SNL. When the results were grouped according to light regime (not divided into intensity), a significant difference in the proportion of the Gaussian-driven  $g_s$  response was observed between SQ- and SN-grown plants (posthoc Tukey,  $P < 0.05$ ), with SQ ( $\sim 17\%$ ) lower than both FL ( $\sim 21\%$ ) and SN ( $25\%$ ) treatments (Fig. 2B). There was no significant difference in the time at which peak  $g_s$  occurred ( $Tm_{sin}$ ) between treatments irrespective of light intensity and treatment (Fig. 2C), except for SNH that took  $\sim 1$  h longer to reach a maximum value of  $g_s$  than all other treatments. Although there was a noticeable trend of FL treatments having lower values of  $Ts_{sin}$  than SN (irrespective of light intensity; Fig. 2D), no significant differences were observed; however,  $Ts_{sin}$  was significantly lower in FL ( $\sim 2.1$  h) than SN ( $\sim 2.35$  h) when grouped by light regime (posthoc Tukey,  $P < 0.05$ ; Fig. 2D). Large variation in the magnitude of the Gaussian element ( $G_{sin}$ ; Fig. 2E) was observed between and within treatments, with values ranging from  $\sim 0.06 \text{ mol m}^{-2} \text{ s}^{-1}$  in SQL to  $\sim 0.15 \text{ mol m}^{-2} \text{ s}^{-1}$  in FLH. SQ-grown plants exhibited lower values of  $G_{sin}$  than FL and SN under both light intensities, with SQL significantly lower (posthoc Tukey,  $P < 0.05$ ) than all other treatments. When light intensities were grouped together, SQ ( $\sim 0.08$ ) grown plants were significantly lower ( $P < 0.05$ ) than FL ( $\sim 0.125$ ) and SN ( $\sim 0.13$ ) treatments (Fig. 2E).

**Figure 2.** Quantification of the Gaussian signal of  $g_s$  during diurnal measurements. Diurnal  $g_s$  measured under square wave light (A); the relative percentage of Gaussian driven  $g_s$  ( $R_{sin}$ , B); the time at which peak  $g_s$  occurs ( $Tm_{sin}$ , C); the width of the peak ( $Ts_{sin}$ , D); and the magnitude of the Gaussian  $g_s$  response ( $G_{sin}$ , E). FLH (red), SNH (green), and SQH (blue) high-light treatments (full lines) were measured under  $SQ_{High}$ . FLL (red), SNL (green), and SQL (blue) low-light treatments (dashed lines) were measured under  $SQ_{Low}$ . Bars are combined data from high and low-light treatments. Error bars represent mean  $\pm$  SE,  $n = 5-7$ . Colored letters represent the results of Tukey's posthoc comparisons of group means from the individual light treatments, and black letters are the result from combined high- and low-light treatments.



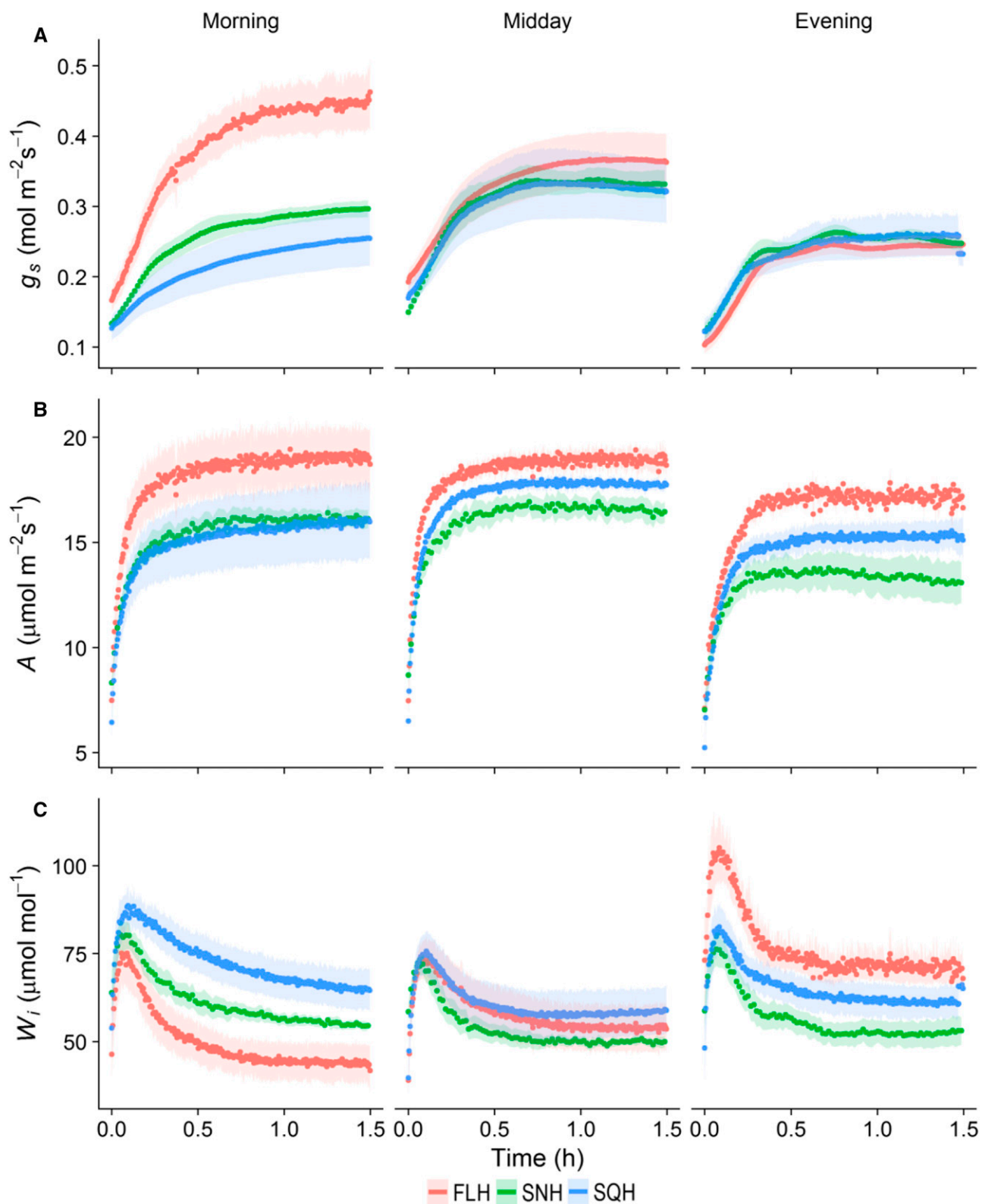


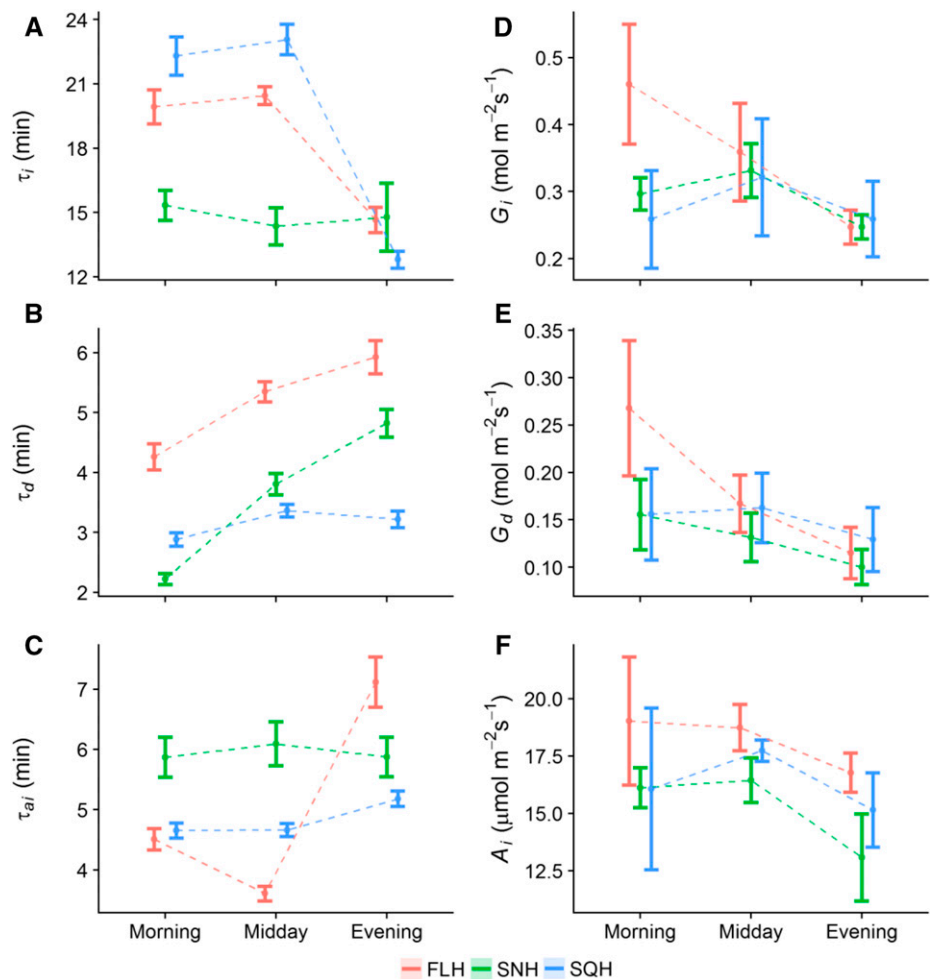
**Figure 3.** Temporal response of  $g_s$ ,  $A$ , and  $W_i$  to a step increase in light intensity (from 100 to 1,000  $\mu\text{mol m}^{-2} \text{s}^{-1}$ ), at different times of the day. Gas exchange parameters ( $g_s$ , A, B; and  $W_i$ , C) were recorded at 20-s intervals, leaf temperature maintained at 25°C, and leaf VPD at  $1 \pm 0.2$  kPa. Plants grown under the three high-light treatments: *FLH* (red); *SNH* (green); *SQH* (blue). Error ribbons represent mean  $\pm$  SE.  $n = 5-6$ .

**Response of  $g_s$  and  $A$  to a Step Change in PPFD as a Function of Time of Day**

To assess the impact of growth light regimes on stomatal responses, leaves were subjected to a step increase in PPFD ( $100\text{--}1,000\ \mu\text{mol m}^{-2}\ \text{s}^{-1}$ ) followed by a step decrease ( $1,000\text{--}100\ \mu\text{mol m}^{-2}\ \text{s}^{-1}$ ), and the effect on  $A$  and  $g_s$  measured using gas exchange. In the morning period (8–10 AM), both high and low intensity fluctuating light treatments (FLH; Fig. 3A; FLL; Supplemental Fig. S1A) and SNH (Fig. 3A; SNL; Supplemental Fig. S1A) reached a new plateau of  $g_s$  within 90 min after the light increase, while both the square wave treatments (SQH; Fig. 3A) and SQL (Supplemental Fig. S1A) failed to reach a new plateau of  $g_s$  within this timeframe. In the midday (1–3 PM) and evening (6–8 PM) measurements,  $g_s$  reached a plateau in all light treatments (high, Fig. 3A; low, Supplemental Fig. S1A) within 90 min. Following the increase in PPFD to  $1,000\ \mu\text{mol m}^{-2}\ \text{s}^{-1}$ , a near instantaneous increase in  $A$  was observed in contrast with the slow initial increase in  $g_s$  in all treatments and at all times of day (Fig. 3B; Supplemental Fig. S1B). In all treatments and three measurement times,  $g_s$  continued to increase during the

measurement period despite the fact that  $A$  had reached near steady-state levels. Although all treatments displayed a predominantly uncoordinated  $A$  and  $g_s$  temporal response, final values of  $A$  and  $g_s$  were strongly correlated, especially in the morning where FLH exhibited the highest levels of operational maximum  $g_s$  and  $A$ , while SQH displayed the lowest values in each category (Fig. 3, A and B).  $W_i$ , measured as  $A/g_s$ , increased over the day in FL-grown plants (Fig. 3C), predominantly driven by the decrease in  $g_s$  values over this period (Fig. 3A).  $W_i$  measured in SQ- and SN-grown plants changed little between morning and evening, although SQ-grown plants always exhibited higher values than SN plants.  $W_i$  values were higher in the morning for SQ- and SN-grown plants compared to FL treatments irrespective of light intensity (Fig. 3C; Supplemental Fig. S1C), driven largely by the lower  $g_s$  values (Fig. 3A). In the evening, the inverse was evident with FL treatments displaying higher levels of  $W_i$  driven by the higher  $A$  values in FLH-grown plants (Fig. 3B) and the lower final  $g_s$  values in FLL-grown plants (Supplemental Fig. S1A). In all treatments, final values of  $g_s$  decreased through the day (morning to

**Figure 4.** Modeled temporal response of  $g_s$  and  $A$  to a step change in light.  $\tau_i$  (A),  $\tau_d$  (B), and  $\tau_{ai}$  (C) to a step change in light intensity (from  $100$  to  $1,000\ \mu\text{mol m}^{-2}\ \text{s}^{-1}$ ; and from  $1,000$  to  $100\ \mu\text{mol m}^{-2}\ \text{s}^{-1}$ , respectively) at different times of the day.  $g_s$  following a step increase in light intensity (from  $100$  to  $1,000\ \mu\text{mol m}^{-2}\ \text{s}^{-1}$ ) ( $G_i$ , D) and after light intensity returned to  $100\ \mu\text{mol m}^{-2}\ \text{s}^{-1}$  ( $G_d$ , E); and light saturated rate of  $A$  at  $1,000\ \mu\text{mol m}^{-2}\ \text{s}^{-1}$  ( $A_i$ , F), at different times of the day (morning, midday, evening). Plants grown under the three high-light treatments: FLH (red), SNH (green), and SQH (blue). Error bars represent 95% confidence intervals.  $n = 5\text{--}6$ .



evening) when subjected to a step decrease in PPFD from 1,000 to 100  $\mu\text{mol m}^{-2} \text{s}^{-1}$  (Supplemental Fig. S2). In the morning period, the highest final values of  $g_s$  at 100  $\mu\text{mol m}^{-2} \text{s}^{-1}$  were shown by FLH ( $\sim 0.26 \text{ mol m}^{-2} \text{s}^{-1}$ ) grown plants, while SNH ( $0.14 \text{ mol m}^{-2} \text{s}^{-1}$ ) displayed the lowest values (Supplemental Fig. S2), which correlated strongly with the final values of  $g_s$  at 1,000 PPFD (Fig. 3A). In the evening period, final values of  $g_s$  were comparable between all treatments (Supplemental Fig. S2).

### Speed of $g_s$ Response to a Step Change in PPFD

Stomatal responses to a step increase in PPFD were used to determine the influence of acclimation to growth light regime and intensity on the speed of  $g_s$  response at different times of the day. Time constants for stomatal opening ( $\tau_i$ , Fig. 4A) in response to a step increase in light were significantly lower (posthoc Tukey,  $P < 0.05$ ) in SNH-grown plants compared with FLH- and SQH-grown plants when measured in the morning. The slower responses observed in the FLH- and SQH-grown plants remained at the midday measurement period; however,  $\tau_i$  dropped significantly ( $P < 0.05$ ) in the evening measurements in both FLH and SQH, indicating a faster response similar to that observed for SNH throughout the day. In low-light treatments,  $\tau_i$  was significantly faster in SNL-grown plants ( $P < 0.05$ ) compared to FLL and SQL at all times of day (Supplemental Fig. S3A), with time constants decreasing at midday in all treatments before returning in the evening to levels comparable to the morning. In contrast to stomatal opening, time constants for stomatal closure ( $\tau_d$ ) significantly increased (posthoc Tukey,  $P < 0.05$ ) through the day (morning to evening) in all FL and SN treatments irrespective of light intensity (Fig. 4B; Supplemental Fig. S3B),

although stomata of SN-grown plants closed in a significantly shorter time (posthoc Tukey,  $P < 0.05$ ) than FL at all times of day. The  $\tau_d$  was maintained at all times of day in SQ-grown plants irrespective of light intensity, while in both FL and SN treatments  $\tau_d$  significantly increased ( $P < 0.05$ ) from morning to evening. In general, stomatal closure was much slower in plants grown under FL than in SN and SQ, with SN  $g_s$  responses slower than SQ in the evening.

The time constant for light saturated rate of carbon assimilation at 1,000  $\mu\text{mol m}^{-2} \text{s}^{-1}$  PPFD ( $\tau_{ai}$ , Fig. 4C; Supplemental Fig. S3C) was determined from the temporal response data (Fig. 3), along with final values of  $g_s$  at 1,000 PPFD for stomatal opening ( $G_i$ , Fig. 4D; Supplemental Fig. S3D), stomatal closure ( $G_d$ , Fig. 4E; Supplemental Fig. S3E), and saturated rates of  $A$  at 1,000 PPFD ( $A_i$ , Fig. 4F; Supplemental Fig. S3F). Net  $\text{CO}_2$  assimilation was deemed saturated at 1,000 PPFD from analysis of light response curves on the same plants (see Vialet-Chabrand et al., 2017b). Time constants for light saturated  $A$  ( $\tau_{ai}$ , Fig. 4C) were significantly higher (posthoc Tukey,  $P < 0.05$ ) in SNH compared to SQH and FLH at morning and midday, while in the evening  $\tau_{ai}$  was significantly higher ( $P < 0.05$ ) in FLH. In low-light treatments (Supplemental Fig. S3C),  $\tau_{ai}$  significantly decreased ( $P < 0.05$ ) from morning to midday in SQL and SNL, and significantly decreased ( $P < 0.05$ ) in all low-light treatments from midday to evening. The final  $g_s$  at 1,000  $\mu\text{mol m}^{-2} \text{s}^{-1}$  ( $G_i$ , Fig. 4D; Supplemental Fig. S3D), and following closure when light was reduced from 1,000 to 100  $\mu\text{mol m}^{-2} \text{s}^{-1}$  ( $G_d$ , Fig. 4E; Supplemental Fig. S3E) differed significantly through the day. Final  $g_s$  at 1,000 PPFD ( $G_i$ ) decreased significantly ( $P < 0.05$ ) from morning to evening in FLH-grown plants ( $\sim 0.46$  to  $0.25 \text{ mol m}^{-2} \text{s}^{-1}$ , respectively; Fig. 4D), whereas SQH and SNH treatments remained constant throughout the day, displaying a trend of increased  $G_i$  at midday. All

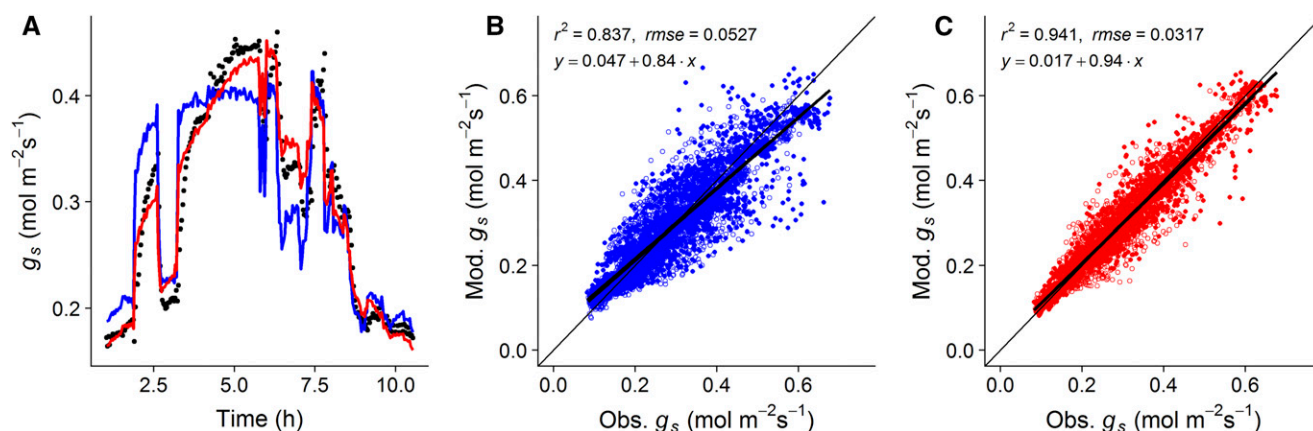


**Figure 5.** Comparison of the Ball-Berry model prediction of  $g_s$  with and without a Gaussian element. An example of adjustment made on an existing independent data set (black circles) measured under a dynamic light environment (A; Vialet-Chabrand et al., 2017b) for the Ball-Berry model without (blue line) and with (red line) a Gaussian element. Shown are the comparisons between measured and predicted  $g_s$  values using the Ball-Berry model without (B; blue dots) and with (C; red dots) a Gaussian element. Open and closed circles are the fluctuating and square-wave treatments, respectively, from the independent data set.

low-light treatments (FLL, SQL, and SNL) displayed similar trends in  $G_i$  throughout the day, with a significant decrease ( $P < 0.05$ ) from morning to evening;  $\sim 0.35$  to  $0.21 \text{ mol m}^{-2} \text{ s}^{-1}$  in FLL;  $\sim 0.34$  to  $0.23 \text{ mol m}^{-2} \text{ s}^{-1}$  in SQL; and  $\sim 0.33$  to  $0.23 \text{ mol m}^{-2} \text{ s}^{-1}$  in SNL (morning and evening, respectively, Supplemental Fig. S3D). Final values of  $g_s$  at 100 PPFD ( $G_i$ ; Fig. 4E; Supplemental Fig. S3E) displayed similar trends to that of  $G_i$  in all treatments, irrespective of light intensity.  $G_d$  significantly decreased ( $P < 0.05$ ) from morning to evening in FLH-grown plants ( $\sim 0.27$  to  $0.11 \text{ mol m}^{-2} \text{ s}^{-1}$ ; Fig. 4E), though remained constant in SQH and SNH treatments at all times of day. In all low-light treatments,  $G_d$  significantly decreased ( $P < 0.05$ ) from morning to evening (Supplemental Fig. S3E);  $\sim 0.17$  to  $0.1 \text{ mol m}^{-2} \text{ s}^{-1}$  in FLL;  $\sim 0.19$  to  $0.13 \text{ mol m}^{-2} \text{ s}^{-1}$  in SQL; and  $\sim 0.15$  to  $0.1 \text{ mol m}^{-2} \text{ s}^{-1}$  in SNL (morning and evening, respectively, Supplemental Fig. S3E). Saturated rates of  $A$  at 1,000 PPFD ( $A_i$ ; Fig. 4F; Supplemental Fig. S3F) remained constant from morning to midday in all treatments, irrespective of light intensity. In all light treatments, there was a decrease in  $A_i$  from midday to evening, although this was significant only in SNH and SQL treatments (posthoc Tukey,  $P < 0.05$ ). A strong correlation was observed in all treatments between the final value of  $g_s$  ( $G_i$ ) and  $A$  ( $A_i$ )  $< 1,000 \mu\text{mol m}^{-2} \text{ s}^{-1}$  PPFD. With regard to stomatal anatomy, significant differences in stomatal density were observed between plants grown under high and low-light intensity, though no difference was observed between plants grown under the different patterns of growth light of the same average intensity (data not shown).

### Impact of Diurnal Stomatal Behavior on Predictive Models of $g_s$ in a Dynamic Environment

The Ball-Berry model (Ball et al., 1987) is widely used in the literature as a basis for predicting  $g_s$  across leaf and global scales (Damour et al., 2010). Based on our findings and having quantified and established the significance of  $g_s$  response over the diurnal period, we investigated whether adding a time of day effect (Gaussian element) to the Ball-Berry model would improve predictive power and model fit when endeavoring to predict  $g_s$  under different light regimes and intensities. To exemplify the improvements in predictive power, and display an example of the fit of the two models (with and without the Gaussian element), we used a completely independent data set (Fig. 5A), measured under a dynamic light environment previously described in Vialet-Chabrand et al. (2017b). By adding a Gaussian element into the Ball-Berry model, our model exhibited improvements in the prediction of  $g_s$  at all times of day, especially at periods of high and low light where the original Ball-Berry model failed to accurately predict the full range of variation in the data (Fig. 5A). Figure 5 shows the difference between measured and predicted  $g_s$  values using the Ball-Berry model without (Fig. 5B) and with (Fig. 5C) a Gaussian element. We observed that under all light conditions

the best model fit was always that with the addition of the Gaussian element.  $R^2$  of the relationship between observed and predicted data increased by over 10% (0.837 to 0.941, respectively), and *rmse* was improved by  $\sim 40\%$  (0.0527 to 0.0317, respectively), indicating a significant improvement in predictive power. This indicates that although the Ball-Berry model and its derivatives have the ability to predict  $g_s$  under different light regimes, the addition of a Gaussian element significantly improves performance, especially under a dynamic light environment.

### DISCUSSION

It is well established that plants acclimate to growth light intensity by altering leaf anatomy and biochemistry as well as physiology (Givnish, 1988; Walters and Horton, 1994; Weston et al., 2000; Bailey et al., 2001, 2004). However, few studies have focused on stomatal acclimation to the pattern of growth light. Although in a recent study we reported photosynthesis and to some extent stomatal conductance acclimate to the pattern and intensity of growth irradiance (Vialet-Chabrand et al., 2017b), this study did not examine how acclimation to fluctuating growth light influences the magnitude and temporal dynamics of  $g_s$  over the diurnal period. Here we demonstrate the impact of fluctuating growth lighting regimes on stomatal behavior and show an acclimation of the rapidity and magnitude of stomatal responses over the day. Additionally, we report a previously undescribed internally driven diurnal signal (referred to as the internal signal) that uncouples  $g_s$  from  $A$ , the magnitude and shape of which were modified by both light intensity and light pattern.

### Effect of Acclimation to Growth Light on Stomatal Kinetics

Similar to previously published work (Gay and Hurd, 1975; Lake et al., 2001), our results showed anatomical stomatal acclimation to light intensity, with significantly higher stomatal density under high light. However, as we found no change in stomatal density between growth treatments of the same intensity, the physiological differences observed and reported here are the result of alterations to guard cell biochemistry, sensitivity, or signaling.

Both the rapidity and magnitude of  $g_s$  responses to a step change in PPFD were influenced by growth light regimes, and this was particularly evident at the start of the day. Plants grown under dynamic (fluctuating and sinusoidal) high light showed a faster response and in general a greater magnitude of change; however, these differences in stomatal responses diminished throughout the day. This has also been described previously by Mencuccini et al. (2000), but not in the context of light acclimation. These authors used detached leaves and pressurized them to simulate different levels of leaf water status, and hypothesized that the magnitude of  $g_s$  responses observed at different times of the day were driven by changes in the osmotic regulation that altered



stomatal aperture. Others have also described a reduction in the magnitude of the  $g_s$  response through time (Pfirsch and Pearcy, 1989; Allen and Pearcy, 2000); however, faster responses toward the end of the day were not reported. In contrast to opening, a slower closing response was observed in plants grown under dynamic light, with slower time constants for closure in the evening compared to the morning. This strategy was described previously by Ooba and Takahashi (2003), and it is believed to improve light use efficiency by maintaining open stomata under fluctuating light, reducing the limitation of  $A$  by  $g_s$ . This may also represent a more conservative strategy in energy (e.g. cost of stomatal movements; Raven, 2014) under fluctuating light regimes.

The decrease over the course of the day in the absolute values of both  $A$  and  $g_s$  (observed in both the measurements following the step increase in light and over the diurnal period) could be attributed to the accumulation of photosynthetic products, resulting in a negative feedback on the Calvin cycle (Paul and Foyer, 2001; Paul and Pellny, 2003), or an increase in apoplastic Suc that accumulates in the guard cells, regulated by the rate of transpiration (Lu et al., 1997; Outlaw 2003; Kang et al., 2007; Kelly et al., 2013; Lawson et al., 2014; Daloso et al., 2016). However, no significant acclimation of the slow decrease in  $A$  and  $g_s$  through the day by growth light intensity and pattern was observed in this experiment.

The acclimation of the rapidity of  $g_s$  response was sensitive to light intensity as well as pattern. Previous studies in forest (Percy, 2007) and crop canopies (Barradas et al., 1994; Qu et al., 2016) have reported stomatal acclimation to different light environments with leaves at different heights or positions within the canopy receiving varying degrees of light intensity (Barradas et al., 1998), resulting in different anatomical and biochemical features (Givnish, 1988; Percy, 2007). In general, under lower light maximum  $g_s$  throughout the day is reduced and the speed of the  $g_s$  response is dependent on species and growth environment (Allen and Pearcy, 2000; Ooba and Takahashi, 2003; Vico et al., 2011; Drake et al., 2013; Violet-Chabrand et al., 2013, 2017a; McAusland et al., 2016). However, to date no study has clearly identified the environmental impact on the rapidity of  $g_s$  response. Here, we quantify for the first time the impact of growth light on the acclimation of the rapidity of the  $g_s$  response at different times of the day. Our results reveal that estimates of the rapidity of  $g_s$  will depend on the microenvironment experienced by the chosen leaf and the time at which the measurement is captured.

As stomatal responses to changing light are an order of magnitude slower than photosynthetic responses (Jones, 1998, 2013; Lawson et al., 2010), slower stomata can limit  $\text{CO}_2$  diffusion for  $A$  (Barradas et al., 1998; Kaiser and Kappen, 2000; McAusland et al., 2016; Violet-Chabrand et al., 2017a; Vico et al., 2011), while higher  $g_s$  can be at the expense of  $W_i$ . The different growth light

regimes clearly elicited different acclimation responses, with plants grown under fluctuating light regimes showing the greatest variation in  $W_i$  throughout the day as observed in the light step measurements.  $W_i$  was lowest in the morning in plants grown under fluctuating light and increased toward the evening. A possible explanation for this could be that although these plants receive the same amount of light as the other treatments throughout the day, the majority of this light was delivered earlier in the day. This suggests that the pattern of light distribution leads to an acclimation that will determine the kinetics and magnitude of the  $g_s$  response at different times of day. Although the stomatal acclimation described here in plants subjected to fluctuating light may show a reduction in the efficiency of water use earlier in the day, it may be important for light utilization of sun/shade flecks for photosynthesis, as previously shown by Violet-Chabrand et al. (2017b) when these plants were measured under their growth light regime. The variation in  $W_i$  over the diurnal period may represent a more conservative strategy that potentially balances  $\text{CO}_2$  uptake and water loss over the diurnal period to optimize the current needs at the whole plant level (Meinzer and Grantz, 1990).

#### Effect of Growth Light Acclimation and the Internal Signal on Diurnal Responses

Diurnal gas exchange under constant light revealed an internally driven diurnal  $g_s$  response that was not only disconnected from  $A$ , but also strongly influenced by the patterns of growth light regime and to a smaller extent the average light intensity. The importance of the internal  $g_s$  response over the diurnal period was unexpected, with ~25% of the total daily  $g_s$  driven by this signal. This diurnal stomatal response could be considered detrimental, as significant water is lost for no extra carbon gain; however, it may also play a valuable role in translocation of photosynthates, nutrient uptake, and/or maintenance of optimal leaf temperature through transpirational cooling (Caird et al., 2007; Hills et al., 2012). Although measured under constant light, all plants showed a characteristic sinusoidal pattern of response of  $g_s$  over the diurnal period similar to that reported by Dodd et al. (2005). What is novel and intriguing about these findings is that  $g_s$  was not only partially uncoupled from  $A$  over a substantial part of the day, but that the characteristics (magnitude and period) of this internal  $g_s$  response are acclimating to the growth light intensity *and* the pattern of the lighting regime.

Previous reports have suggested that such oscillations in  $g_s$  are entrained by circadian rhythms (Dodd et al., 2004; Hubbard and Webb, 2015; Resco de Dios et al., 2016; Hassidim et al., 2017). However, characterization of this response as circadian would require continuous measurements over multiple days (3+ days) in a constant low-light environment to establish if the rhythm persists in each theoretical diurnal time period (Dodd et al., 2005). It is well established that regulation of temporal transcription

patterns by the circadian clock play an important role in rhythms of photosynthesis and stomatal opening (Dodd et al., 2004, 2005; Hubbard and Webb, 2015; Hassidim et al., 2017), although the pathways and signals that lead to this diurnal behavior in  $g_s$  are still largely unknown. Some hypotheses involving ABA concentration (Mencuccini et al., 2000; Tallman, 2004) and the level of Suc and calcium signaling (Dodd et al., 2006; Haydon et al., 2017) have been put forward to explain internally driven diurnal variations in  $g_s$ .

Quantifying the impact of growth environment and acclimation on these patterns and physiological responses under environmentally relevant conditions is extremely difficult. To address this, we built a diurnal model of  $g_s$  that allowed us to quantify this internal signal as well as the influence of lighting regimes on the magnitude and periodicity. This model was accurate ( $R^2$  0.99) at describing the response of  $g_s$ , and the parameters derived from this model allowed us to quantify the relative importance of the internal signal on  $g_s$ . Plants grown under dynamic light regimes showed a higher magnitude of  $g_s$  response under constant light conditions, which highlights the importance of growth light pattern on the acclimation of this internal signal. Interestingly, the duration of the  $g_s$  response to the internal signal was also dependent on growth light regime. These large changes in  $g_s$  over the course of the day represent a significant loss in water with little variation in  $\text{CO}_2$  assimilation over the same period, resulting in significantly reduced plant  $W_i$ . This emphasizes the importance of the growth light regime as it potentially influences the regulation of  $g_s$  by an internal signal that may be under the control of the circadian clock and alters  $g_s$  over the course of the day.

### Implications of the Internal Signal on the Ball-Berry Model

Our results revealed that diurnal stomatal behavior is influenced by the pattern and intensity of growth light, but this is often ignored in current steady-state models of  $g_s$  (Damour et al., 2010). Here, we demonstrate that the addition of an equation describing the internal signal to the widely used Ball-Berry model (Ball et al., 1987) greatly improves the predictive power of the model. Using this new model and an independent data set (Violet-Chabrand et al., 2017b) measured under a dynamic environment, we showed improvements in both the  $R^2$  (~10%) and a reduction in the error (*rmse*; ~40%) between observed and predicted data, highlighting the importance of this process under dynamic fluctuating light. Although integration of a diurnal signal to the Ball-Berry model was first attempted by Resco de Dios et al. (2016) and also showed an improvement in the prediction of  $g_s$ , here, we provide a more precise validation of our model with higher time resolution that enables us to capture rapid variations under fluctuating light regimes. The unexplained variance by the new model may be due to

changes in the rapidity and magnitude of stomatal response at different times of the day, as we have shown experimentally here, but could not be integrated due to the steady-state nature of the Ball-Berry model. To further improve model predictions, a dynamic model that can integrate our findings will be required that not only includes the diurnal/circadian regulation of  $g_s$  but altered  $g_s$  kinetics at different times of day.

### CONCLUSION

In this study, we directly examined the impact of dynamic growth light regimes on stomatal acclimation and diurnal behavior. We have demonstrated that growth light environment modifies stomatal kinetics at different times of the day, resulting in differences in the rapidity and magnitude of this response. Importantly, we also describe and quantify the response to an internal signal that uncouples  $A$  and  $g_s$  over the majority of the diurnal period, with characteristics that are modified by growth light environment. The importance of this signal on diurnal  $g_s$  kinetics is demonstrated by the inclusion of the Gaussian element describing the internal signal, which greatly improves the prediction of  $g_s$  from the widely used Ball-Berry model.

Our quantification of the components of the diurnal kinetic of  $g_s$  (response to light, gradual temporal decrease, and Gaussian element) provides an invaluable tool for assessing diurnal patterns of stomatal behavior, as well as the effect of the circadian clock. A dynamic model of  $g_s$  that includes these components will be able to describe the contribution of each element to the diurnal response of  $g_s$ , even under a dynamic environment such as that experienced by plants in the field. This has been illustrated by the improvement in predicted  $g_s$  from plants acclimated to different light environments and measured under dynamic regimes.

Acclimation of the rapidity and response of  $g_s$  to the internal signal appears to be determined by both the intensity and pattern of growth light, and is an important strategy for maintaining carbon fixation and overall plant water status by conditioning the plant to respond appropriately to future diurnal variations in light.

### MATERIALS AND METHODS

#### Plant Material and Growth Conditions

Fluctuating and square wave light growth conditions were delivered via a Heliospectra L4A LED light source. Fluctuating light regime ( $FL_{High}$ ) was recreated from a natural light regime recorded at the University of Essex during a relatively clear day in July (Fig. 1; with the assumption of a constant spectral distribution). The average light intensity over the 12-h fluctuating regime was calculated as  $460 \mu\text{mol m}^{-2} \text{s}^{-1}$  and was used as the light intensity for the square wave high-light treatment ( $SQ_{High}$ ). This value was then halved to  $230 \mu\text{mol m}^{-2} \text{s}^{-1}$  for the fluctuating ( $FL_{Low}$ ) and square wave ( $SQ_{Low}$ ) low-light conditions. Plants (*Arabidopsis* [*Arabidopsis thaliana*] Col-0) were grown in peat-based compost (Levingtons F25; Everris) and were maintained under well-watered conditions in a

controlled environment, with growth conditions maintained at a relative humidity of 55% to 65%, air temperature of 21–22°C, and a CO<sub>2</sub> concentration of 400 μmol mol<sup>-1</sup>. The position of the plants under the light source was changed daily at random to remove any effect of potential heterogeneity in the light quality and quantity.

### Simulating Daily Light Fluctuations for Sinusoidal Growth Light Regime

The sinusoidal light regime was simulated using a specific algorithm including a sinusoidal variation with random alterations constrained to maintain the daily amount of light intensity (PPFD) constant during the growth. The sinusoidal variation as a function of time (*t*) was obtained by:

$$PPFD = ae^{-\frac{(t-b)^2}{2c^2}} - ae^{-\frac{(t-b)^2}{2c^2}} \quad (1)$$

where *a* is the maximum PPFD reached during the peak, *b* is the time at which the peak is reached, and *c* a parameter related to the width of the peak. The value of *a* was arbitrarily set to 1,000 for convenience as the whole curve is rescaled at the final step of the algorithm. Values of *b* and *c* were set to 7 and 13, respectively.

A random number of decreases in light intensity at different times throughout the diurnal period were then added, and ranged between 0 and 80% of the original light level. This guaranteed a minimum light intensity that mimics the daily variation of diffuse light intensity.

The final step was to scale the curve to obtain an average light intensity of 460 μmol m<sup>-2</sup> s<sup>-1</sup> for the sinusoidal high-light treatment (*SN<sub>High</sub>*) and 230 μmol m<sup>-2</sup> s<sup>-1</sup> for the sinusoidal low-light treatment (*SN<sub>Low</sub>*) as used in the other growth light regimes described previously. The same process was repeated for the number of days required and was then programmed into the Heliospectra lights. The first 5 d simulated are shown in Supplemental Figure S4, highlighting that each day had a unique pattern of light intensity, mimicking a natural light environment.

### Leaf Gas Exchange

All gas exchange (*A* and *g<sub>s</sub>*) parameters were recorded using a Li-Cor 6400XT portable gas exchange system, with light delivered via a Li-Cor 6400-40 fluorometer head unit. For all gas exchange measurements, a constant flow rate was set at 300 μmol s<sup>-1</sup>, with cuvette conditions maintained at a CO<sub>2</sub> concentration of 400 μmol mol<sup>-1</sup>, a leaf temperature of 25°C (unless otherwise stated), and to maintain a leaf to air water vapor pressure deficit of 1 (±0.2) kPa, the system was connected to a Li-Cor 610 portable dew point generator. All measurements were taken using the youngest, fully expanded leaf. Intrinsic water use efficiency was calculated as *W<sub>i</sub>* = *A/g<sub>s</sub>*.

### Measurements and Modeling of Diurnal Stomatal Conductance under Constant Light Environment

On the day of measurement, plants were removed from the growth chamber prior to the initiation of the diurnal regime of light. Leaves were placed in the Li-Cor cuvette (for conditions see above) in darkness, and both *A* and *g<sub>s</sub>* were allowed to stabilize for a minimum of 15 to 30 min. After *A* and *g<sub>s</sub>* were at steady state for at least 5 min (<2% change over this time period), the automatic 12-h light programs (*SQ<sub>High</sub>* and *SQ<sub>Low</sub>*) were started, with *A* and *g<sub>s</sub>* recorded every 2 min.

The temporal response of *g<sub>s</sub>* to external and internal cues was modeled using an exponential equation:

$$\frac{dg_s}{dt} = \frac{(G - g_s)}{\tau} \quad (2)$$

where *G* represents the steady-state target of *g<sub>s</sub>* and *τ* the time constant to reach 63% of *G*. Due to the asymmetry of response during a step increase or decrease in light intensity, a different value of *τ* was used in each condition (*τ<sub>i</sub>* and *τ<sub>d</sub>*).

The steady-state target (*G*) was calculated as the sum of three processes: the decrease of *g<sub>s</sub>* through the diurnal period (*D*), the bell shape variation of *g<sub>s</sub>* through the diurnal period (*S*), and the response of *g<sub>s</sub>* to light intensity variation (*G<sub>1</sub>*, *G<sub>2</sub>*, *G<sub>3</sub>*).

Before and after the lighted period, *G* was set to *G<sub>1</sub>* and *G<sub>3</sub>*, respectively, two values representing the steady-state *g<sub>s</sub>* at the end and beginning of the dark

period (gray area in Fig. 1). During the lighted period, *G* was set to *G<sub>2</sub>* + *D* + *S*, assuming that the internal cues were activated by light.

The decrease of *g<sub>s</sub>* (*D*) as a function of time (*t*) was modeled using an exponential function constrained over the lighted portion of the diurnal period (between *t<sub>on</sub>* and *t<sub>off</sub>*):

$$D = \begin{cases} G_{sl} \left( 1 - e^{-\frac{t-t_{on}}{\tau_{sl}}} \right), & \text{if } t > t_{on} \text{ and } t < t_{off} \\ 0, & \text{if } t < t_{on} \text{ and } t > t_{off} \end{cases} \quad (3)$$

where *G<sub>sl</sub>* is the steady-state target of the decrease in *g<sub>s</sub>* and *τ<sub>sl</sub>* the time constant to reach 63% of *G<sub>sl</sub>*.

The bell shape variation of *g<sub>s</sub>* (*S*) as a function of time (*t*) was modeled using a Gaussian function:

$$S = G_{sin} e^{-\frac{(t-Tm_{sin})^2}{(2T_{sin})^2}} \quad (4)$$

where *G<sub>sin</sub>* is the maximum *g<sub>s</sub>* reached during the peak, *Tm<sub>sin</sub>* the time at the center of the peak, and *T<sub>sin</sub>* a parameter related to the width of the peak. On each parameter, a one-way ANOVA with light treatment as factor was applied with a Tukey's posthoc test for comparing group means. Statistics were conducted using R statistical software (version 3.2.4).

This model was implemented using the stan language and adjusted on the observation using R ([www.r-project.org](http://www.r-project.org)) and the RStan package (<http://mc-stan.org/users/interfaces/rstan>). For each diurnal curve of *g<sub>s</sub>* measured, the model was adjusted using three chains starting with different parameter sets. No divergent transitions were observed, meaning that the simulations can be trusted, and Rhat values were all ~1, meaning that all three chains converged (Carpenter et al., 2016).

### Temporal Response of *A* and *g<sub>s</sub>*

For the step change in light, leaves were placed in the Li-Cor cuvette (for conditions, see above) and equilibrated at a PPFD of 100 μmol m<sup>-2</sup> s<sup>-1</sup> until both *A* and *g<sub>s</sub>* were at steady state. Steady state in this case was defined as less than a 2% change of the given parameter over a 10-min period (this would take ~20–60 min). Once at steady state, PPFD was increased to 1,000 μmol m<sup>-2</sup> s<sup>-1</sup> for 1.5 h before returning to 100 μmol m<sup>-2</sup> s<sup>-1</sup> for an additional 1 h. *A* and *g<sub>s</sub>* were recorded every 20 s. For measurements at the different times of day (morning, midday, and evening), plants were removed from the growth chamber at 8 AM, 1 PM, and 6 PM, and the increase in PPFD from 100 to 1,000 μmol m<sup>-2</sup> s<sup>-1</sup> was initiated at ~9 AM, 2 PM, and 7 PM, respectively. To prevent previous step changes in light (e.g. morning) having an effect on the response to step changes later in the day (e.g. midday), individual leaves that were subjected to a step change in light were not subjected to another measurement until the following day.

### Modeling Rapidity of the Stomatal Conductance Response

The rapidity of the stomatal response following a step change in light intensity was assessed as a function of time (*t*) using a custom exponential equation including a slow linear increase of the steady-state target (*G*):

$$g_s = (G + S_1 t) + (g_0 - (G + S_1 t)) e^{-t/\tau} \quad (5)$$

where *S<sub>1</sub>* is the slope of the slow linear increase of *G* observed during the response, *g<sub>0</sub>* the initial value of *g<sub>s</sub>*, and *τ* the time constant to reach 63% of *G* (when *τ* = *t*,  $\frac{G_0 - g_0}{(G + S_1 t) - g_0} = 1 - e^{-1} \sim 0.63$ ). Due to the asymmetry of response during a step increase or decrease in light intensity, a different value of *τ* was used in each condition (*τ<sub>i</sub>* and *τ<sub>d</sub>*). Even if *g<sub>s</sub>* did not reach a plateau within the given timeframe, the model was able to predict the final asymptotic response and therefore the time constant (*τ<sub>i</sub>* and *τ<sub>d</sub>*). This equation was adjusted on response curves of each treatment at different times of the day using a nonlinear mixed effect model. Parameter *G*, *g<sub>0</sub>* and *S<sub>1</sub>* were assumed to vary at individual level (random effects) and *τ* was assumed to vary only at treatment level (fixed effect). R and the nlme package were used to perform the analysis. On each parameter, a one-way ANOVA with light treatment as factor was applied with a Tukey's posthoc test for comparing group means. Confidence intervals at 95% were reported at the treatment level.

## Modeling Rapidity of the Net CO<sub>2</sub> Assimilation Response

The rapidity of the photosynthesis response following a step change in light intensity was assessed as a function of time ( $t$ ) using an updated version of Equation 5:

$$A_t = (A_s + S_1 t) + (A_0 - (A_s + S_1 t))e^{-t/\tau} \quad (6)$$

where  $A_t$  is the net CO<sub>2</sub> assimilation ( $A$ ) at time  $t$ ,  $A_s$  is the plateau of  $A$  reached in steady state,  $S_1$  is the slope of the slow linear increase of  $A$ ,  $A_0$  the initial value of  $A$ , and  $\tau$  the time constant to reach 63% of  $A_s$ . This equation was adjusted on response curves using the same method described above for  $g_s$ .

## Including Variation in Diurnal Stomatal Behavior in the Ball-Berry Model for Predicting $g_s$

An addition was made to the original Ball-Berry model (Ball et al., 1987) to take into consideration the time of the day ( $t$ ) effect on  $g_s$ :

$$g_s = g_0 + \left( g_1 \frac{AH_s}{C_s} \right) + \left( g_2 e^{-\frac{(t-T_m)^2}{2T_s^2}} \right) \quad (7)$$

where  $g_0$  is the minimal conductance or intercept,  $g_1$  the slope of the relationship between  $g_s$  and the Ball index ( $AH_s/C_s$ ),  $g_2$  the amplitude of the Gaussian function,  $T_m$  the time to reach the peak of the Gaussian,  $T_s$  a parameter related to the width of the peak, and  $A$  the net CO<sub>2</sub> assimilation. The conditions imposed at the surface of the leaf are represented by  $H_s$ , the relative humidity, and  $C_s$ , the CO<sub>2</sub> concentration in the chamber.

Using R and the nls function, two versions (with and without the third term in Equation 6) were adjusted on an independent dataset described previously in Viale-Chabrand et al. (2017b). The fluctuating light regime and different light intensities applied on plants grown in different conditions give a large range of variation to test the performance of the Ball-Berry model against our modified version.

The difference between observation (*Obs.*) and predictions (*Mod.*) of both models were assessed using the root mean square error (*rmse*):

$$rmse = \sqrt{\frac{\sum (Obs. - Mod.)^2}{n}} \quad (8)$$

where  $n$  represents the number of recorded data.

## Supplemental Data

The following supplemental materials are available.

**Supplemental Figure S1.** Temporal response of  $g_s$ ,  $A$ , and  $W_i$  to a step increase in light intensity (from 100 to 1,000  $\mu\text{mol m}^{-2} \text{s}^{-1}$ ) at different times of the day for the three low-light treatments.

**Supplemental Figure S2.** Temporal response of  $g_s$  to a step decrease in light intensity (from 1,000 to 100  $\mu\text{mol m}^{-2} \text{s}^{-1}$ ) at different times of the day for all six light treatments.

**Supplemental Figure S3.** Time constants for  $\tau_v$ ,  $\tau_{di}$ , and the light saturated rate of carbon assimilation ( $\tau_{di}$ ) following a step change in light intensity at different times of the day for the three low-light treatments.

**Supplemental Figure S4.** First 5 d of the simulated  $SN_{High}$  highlighting the random fluctuations in light intensity unique to each day.

Received December 22, 2017; accepted January 18, 2018; published January 25, 2018.

## LITERATURE CITED

Allen MT, Percy RW (2000) Stomatal behavior and photosynthetic performance under dynamic light regimes in a seasonally dry tropical rain forest. *Oecologia* **122**: 470–478

Alter P, Dreissen A, Luo FL, Matsubara S (2012) Acclimatory responses of *Arabidopsis* to fluctuating light environment: comparison of different sunfleck regimes and accessions. *Photosynth Res* **113**: 221–237

Assmann SM, Wang XQ (2001) From milliseconds to millions of years: guard cells and environmental responses. *Curr Opin Plant Biol* **4**: 421–428

Bailey S, Horton P, Walters RG (2004) Acclimation of *Arabidopsis thaliana* to the light environment: the relationship between photosynthetic function and chloroplast composition. *Planta* **218**: 793–802

Bailey S, Walters RG, Jansson S, Horton P (2001) Acclimation of *Arabidopsis thaliana* to the light environment: the existence of separate low light and high light responses. *Planta* **213**: 794–801

Ball JT, Woodrow IE, Berry JA (1987) A model predicting stomatal conductance and its contribution to the control of photosynthesis under different environmental conditions. In J Biggins, eds, *Progress in Photosynthesis Research*. Springer, Dordrecht, The Netherlands, pp 221–224

Barradas VL, Jones HG, Clark JA (1994) Stomatal responses to changing irradiance in *Phaseolus vulgaris* L. *J Exp Bot* **45**: 931–936

Barradas VL, Jones HG, Clark JA (1998) Sunfleck dynamics and canopy structure in a *Phaseolus vulgaris* L. canopy. *Int J Biometeorol* **42**: 34–43

Buckley TN (2017) Modeling stomatal conductance. *Plant Physiol* **174**: 572–582

Caird MA, Richards JH, Donovan LA (2007) Nighttime stomatal conductance and transpiration in C3 and C4 plants. *Plant Physiol* **143**: 4–10

Caldeira CF, Jeanguenin L, Chaumont F, Tardieu F (2014) Circadian rhythms of hydraulic conductance and growth are enhanced by drought and improve plant performance. *Nat Commun* **5**: 5365

Carpenter B, Gelman A, Hoffman M, Lee D, Goodrich B, Betancourt M, Brubaker M, Guo J, Li P, Riddell A (2016) Stan: a probabilistic programming language. *J Stat Softw* **20**: 1–37

Chazdon RL, Percy RW (1991) The importance of sunflecks for forest understory plants. *Bioscience* **41**: 760–766

Daloso DM, Dos Anjos L, Fernie AR (2016) Roles of sucrose in guard cell regulation. *New Phytol* **211**: 809–818

Damour G, Simonneau T, Cochard H, Urban L (2010) An overview of models of stomatal conductance at the leaf level. *Plant Cell Environ* **33**: 1419–1438

Dodd AN, Jakobsen MK, Baker AJ, Telzerow A, Hou SW, Laplaze L, Barrot L, Poethig RS, Haseloff J, Webb AA (2006) Time of day modulates low-temperature Ca signals in *Arabidopsis*. *Plant J* **48**: 962–973

Dodd AN, Parkinson K, Webb AA (2004) Independent circadian regulation of assimilation and stomatal conductance in the *ztl-1* mutant of *Arabidopsis*. *New Phytol* **162**: 63–70

Dodd AN, Salathia N, Hall A, Kévei E, Tóth R, Nagy F, Hibberd JM, Millar AJ, Webb AA (2005) Plant circadian clocks increase photosynthesis, growth, survival, and competitive advantage. *Science* **309**: 630–633

Drake PL, Froend RH, Franks PJ (2013) Smaller, faster stomata: scaling of stomatal size, rate of response, and stomatal conductance. *J Exp Bot* **64**: 495–505

Farquhar GD, Sharkey TD (1982) Stomatal conductance and photosynthesis. *Annu Rev Plant Physiol* **33**: 317–345

Fujita T, Noguchi K, Terashima I (2013) Apoplastic mesophyll signals induce rapid stomatal responses to CO<sub>2</sub> in *Commelina communis*. *New Phytol* **199**: 395–406

Gay AP, Hurd RG (1975) The influence of light on stomatal density in the tomato. *New Phytol* **75**: 37–46

Givnish TJ (1988) Adaptation to sun and shade: a whole-plant perspective. *Aust J Plant Physiol* **15**: 63–92

Gorton HL, Williams WE, Assmann SM (1993) Circadian rhythms in stomatal responsiveness to red and blue light. *Plant Physiol* **103**: 399–406

Gorton HL, Williams WE, Binns ME, Gemmill CN, Leheny EA, Shepherd AC (1989) Circadian stomatal rhythms in epidermal peels from *Vicia faba*. *Plant Physiol* **90**: 1329–1334

Hassidim M, Dakhiya Y, Turjeman A, Hussien D, Shor E, Anidjar A, Goldberg K, Green RM (2017) CIRCADIEN CLOCK ASSOCIATED 1 (CCA1) and the circadian control of stomatal aperture. *Plant Physiol* **175**: 1864–1877

Haydon MJ, Mielczarek O, Frank A, Román Á, Webb AAR (2017) Sucrose and ethylene signaling interact to modulate the circadian clock. *Plant Physiol* **175**: 947–958

Hills A, Chen ZH, Amtmann A, Blatt MR, Lew VL (2012) OnGuard, a computational platform for quantitative kinetic modeling of guard cell physiology. *Plant Physiol* **159**: 1026–1042

Hubbard KE, Webb AAR (2015) Circadian rhythms in stomata: physiological and molecular aspects. In SMancuso, SSHabala, eds, *Rhythms in Plants*. Springer International Publishing, Cham, Switzerland, pp 231–255

Jones HG (1998) Stomatal control of photosynthesis and transpiration. *J Exp Bot* **49**: 387–398

- Jones HG (2013) *Plants and Microclimate: A Quantitative Approach to Environmental Plant Physiology*. Cambridge University Press, Cambridge, UK
- Kaiser E, Matsubara S, Harbinson J, Heuvelink E, Marcelis LF (2017b) Acclimation of photosynthesis to lightflecks in tomato leaves: interaction with progressive shading in a growing canopy. *Physiol Plant* <http://dx.doi.org/>
- Kaiser E, Morales A, Harbinson J (2017a) Fluctuating light takes crop photosynthesis on a rollercoaster ride. *Plant Physiol* <http://dx.doi.org/>
- Kaiser E, Morales A, Harbinson J, Heuvelink E, Prinzenberg AE, Marcelis LFM (2016) Metabolic and diffusional limitations of photosynthesis in fluctuating irradiance in *Arabidopsis thaliana*. *Sci Rep* **6**: 31252
- Kaiser H, Kappen L (2000) In situ observation of stomatal movements and gas exchange of *Aegopodium podagraria* L. in the understorey. *J Exp Bot* **51**: 1741–1749
- Kang Y, Outlaw WH Jr, Andersen PC, Fiore GB (2007) Guard-cell apoplastic sucrose concentration—a link between leaf photosynthesis and stomatal aperture size in the apoplastic phloem loader *Vicia faba* L. *Plant Cell Environ* **30**: 551–558
- Katul GG, Oren R, Manzoni S, Higgins C, Parlange MB (2012) Evapotranspiration: a process driving mass transport and energy exchange in the soil-plant-atmosphere-climate system. *Rev Geophys* **50**: RG3002
- Kelly G, Moshelion M, David-Schwartz R, Halperin O, Wallach R, Attia Z, Belausov E, Granot D (2013) Hexokinase mediates stomatal closure. *Plant J* **75**: 977–988
- Kirschbaum MUF, Gross LJ, Pearcy RW (1988) Observed and modelled stomatal responses to dynamic light environments in the shade plant *Alocasia macrorrhiza*. *Plant Cell Environ* **11**: 111–121
- Kromdijk J, Głowacka K, Leonelli L, Gabilly ST, Iwai M, Niyogi KK, Long SP (2016) Improving photosynthesis and crop productivity by accelerating recovery from photoprotection. *Science* **354**: 857–861
- Külheim C, Agren J, Jansson S (2002) Rapid regulation of light harvesting and plant fitness in the field. *Science* **297**: 91–93
- Lake JA, Quick WP, Beerling DJ, Woodward FI (2001) Plant development. Signals from mature to new leaves. *Nature* **411**: 154
- Lawson T, Blatt MR (2014) Stomatal size, speed, and responsiveness impact on photosynthesis and water use efficiency. *Plant Physiol* **164**: 1556–1570
- Lawson T, Simkin AJ, Kelly G, Granot D (2014) Mesophyll photosynthesis and guard cell metabolism impacts on stomatal behaviour. *New Phytol* **203**: 1064–1081
- Lawson T, von Caemmerer S, Baroli I (2010) Photosynthesis and stomatal behaviour. In UE Lüttge, W Beyschlag, B Büdel, D Francis, eds, *Progress in Botany*. Springer, Berlin, Heidelberg, pp 265–304
- Lee J, Bowling DJF (1992) Effect of the mesophyll on stomatal opening in *Commelina communis*. *J Exp Bot* **43**: 951–957
- Lu P, Outlaw WH Jr, Smith BG, Freed GA (1997) A new mechanism for the regulation of stomatal aperture size in intact leaves: accumulation of mesophyll-derived sucrose in the guard-cell wall of *Vicia faba*. *Plant Physiol* **114**: 109–118
- Matthews JSA, Violet-Chabrand SRM, Lawson T (2017) Diurnal variation in gas exchange: the balance between carbon fixation and water loss. *Plant Physiol* **174**: 614–623
- McAusland L, Davey PA, Kanwal N, Baker NR, Lawson T (2013) A novel system for spatial and temporal imaging of intrinsic plant water use efficiency. *J Exp Bot* **64**: 4993–5007
- McAusland L, Violet-Chabrand S, Davey P, Baker NR, Brendel O, Lawson T (2016) Effects of kinetics of light-induced stomatal responses on photosynthesis and water-use efficiency. *New Phytol* **211**: 1209–1220
- Meinzer FC, Grantz DA (1990) Stomatal and hydraulic conductance in growing sugarcane: stomatal adjustment to water transport capacity. *Plant Cell Environ* **13**: 383–388
- Mencuccini M, Mambelli S, Comstock J (2000) Stomatal responsiveness to leaf water status in common bean (*Phaseolus vulgaris* L.) is a function of time of day. *Plant Cell Environ* **23**: 1109–1118
- Morison JIL (2003) Plant water use, stomatal control. In BA Stewart, TA Howell, eds, *Encyclopedia of Water Science*. Marcel Dekker, New York, pp 680–685
- Morison JIL, Baker NR, Mullineaux PM, Davies WJ (2008) Improving water use in crop production. *Philos Trans R Soc Lond B Biol Sci* **363**: 639–658
- Mott KA, Sibbersen ED, Shope JC (2008) The role of the mesophyll in stomatal responses to light and CO<sub>2</sub>. *Plant Cell Environ* **31**: 1299–1306
- Ohara T, Satake A (2017) Photosynthetic entrainment of the circadian clock facilitates plant growth under environmental fluctuations: perspectives from an integrated model of phase oscillator and phloem transportation. *Front Plant Sci* **8**: 1859
- Ooba M, Takahashi H (2003) Effect of asymmetric stomatal response on gas-exchange dynamics. *Ecol Modell* **164**: 65–82
- Outlaw WH (2003) Integration of cellular and physiological functions of guard cells. *CRC Crit Rev Plant Sci* **22**: 503–529
- Paul MJ, Foyer CH (2001) Sink regulation of photosynthesis. *J Exp Bot* **52**: 1383–1400
- Paul MJ, Pellny TK (2003) Carbon metabolite feedback regulation of leaf photosynthesis and development. *J Exp Bot* **54**: 539–547
- Pearcy R (2007) Responses of plants to heterogeneous light environments. In F Valladares, F Pugnaire, eds, *Functional Plant Ecology*, Ed 2. Boca Raton, London, New York, CRC Press, pp 213–246
- Pearcy RW (1990) Photosynthesis in plant life. *Annu Rev Plant Physiol Plant Mol Biol* **41**: 421–453
- Pfitsch WA, Pearcy RW (1989) Daily carbon gain by *Adenocaulon bicolor* (Asteraceae), a redwood forest understorey herb, in relation to its light environment. *Oecologia* **80**: 465–470
- Poorter H, Fiorani F, Pieruschka R, Wojciechowski T, van der Putten WH, Kleyer M, Schurr U, Postma J (2016) Pampered inside, pestered outside? Differences and similarities between plants growing in controlled conditions and in the field. *New Phytol* **212**: 838–855
- Qu M, Hamdani S, Li W, Wang S, Tang J, Chen Z, Song Q, Li M, Zhao H, Chang T, et al (2016) Rapid stomatal response to fluctuating light: an under-explored mechanism to improve drought tolerance in rice. *Funct Plant Biol* **43**: 727–738
- Raven JA (2014) Speedy small stomata? *J Exp Bot* **65**: 1415–1424
- Resco de Dios V, Gessler A, Ferrio JP, Alday JG, Bahn M, Del Castillo J, Devidal S, García-Muñoz S, Kayler Z, Landais D, et al (2016) Circadian rhythms have significant effects on leaf-to-canopy scale gas exchange under field conditions. *Gigasci* **5**: 43
- Seki M, Ohara T, Hearn TJ, Frank A, da Silva VCH, Caldana C, Webb AAR, Satake A (2017) Adjustment of the *Arabidopsis* circadian oscillator by sugar signalling dictates the regulation of starch metabolism. *Sci Rep* **7**: 8305
- Suorsa M, Järvi S, Grieco M, Nurmi M, Pietrzykowska M, Rantala M, Kangasjärvi S, Paakkari V, Tikkanen M, Jansson S, et al (2012) PROTON GRADIENT REGULATION5 is essential for proper acclimation of *Arabidopsis* photosystem I to naturally and artificially fluctuating light conditions. *Plant Cell* **24**: 2934–2948
- Tallman G (2004) Are diurnal patterns of stomatal movement the result of alternating metabolism of endogenous guard cell ABA and accumulation of ABA delivered to the apoplast around guard cells by transpiration? *J Exp Bot* **55**: 1963–1976
- Tinoco-Ojanguren C, Pearcy RW (1993) Stomatal dynamics and its importance to carbon gain in two rainforest Piper species: II. Stomatal versus biochemical limitations during photosynthetic induction. *Oecologia* **94**: 395–402
- Violet-Chabrand S, Dreyer E, Brendel O (2013) Performance of a new dynamic model for predicting diurnal time courses of stomatal conductance at the leaf level. *Plant Cell Environ* **36**: 1529–1546
- Violet-Chabrand S, Matthews JSA, Simkin AJ, Raines CA, Lawson T (2017b) Importance of fluctuations in light on the acclimation of *Arabidopsis thaliana*. *Plant Physiol* **173**: 2163–2179
- Violet-Chabrand SRM, Matthews JSA, McAusland L, Blatt MR, Griffiths H, Lawson T (2017a) Temporal dynamics of stomatal behavior: modeling and implications for photosynthesis and water use. *Plant Physiol* **174**: 603–613
- Vico G, Manzoni S, Palmroth S, Katul G (2011) Effects of stomatal delays on the economics of leaf gas exchange under intermittent light regimes. *New Phytol* **192**: 640–652
- Walters R, Horton P (1994) Acclimation of *Arabidopsis thaliana* to the light environment: changes in composition of the photosynthetic apparatus. *Planta* **195**: 248–256
- Way DA, Pearcy RW (2012) Sunflecks in trees and forests: from photosynthetic physiology to global change biology. *Tree Physiol* **32**: 1066–1081
- Weston E, Thorogood K, Vinti G, López-Juez E (2000) Light quantity controls leaf-cell and chloroplast development in *Arabidopsis thaliana* wild type and blue-light-perception mutants. *Planta* **211**: 807–815
- Wong SC, Cowan IR, Farquhar GD (1979) Stomatal conductance correlates with photosynthetic capacity. *Nature* **282**: 424–426
- Yamori W (2016) Photosynthetic response to fluctuating environments and photoprotective strategies under abiotic stress. *J Plant Res* **129**: 379–395
- Yin ZH, Johnson GN (2000) Photosynthetic acclimation of higher plants to growth in fluctuating light environments. *Photosynth Res* **63**: 97–107